Solvent Effects on the Suppression of Oxidative Decomposition of Guanines by Phenyl Group Attachment in Deoxyribonucleic Acid (DNA)

Satoshi Yokojima,[†,‡] Wataru Yanoi,[‡] Norifumi Yoshiki,[‡] Noriyuki Kurita,[§] Shigenori Tanaka,[⊥] Kazuhiko Nakatani,[†,||] and Akira Okada*[,‡]

Japan Science and Technology Corporation (JST), 4-1-8 Honcho, Kawaguchi 332-0012, Japan, Institute of Materials Science, University of Tsukuba, 1-1-1, Ten-nodai, Tsukuba 305-8573, Japan, Department of Knowledge-Based, Information Engineering, Toyohashi University of Technology, Tempaku-cho, Toyohashi 441-8580, Japan, Advanced Materials and Devices Laboratory, Toshiba R&D Center, Kawasaki 212-8582, Japan, Department of Synthetic Chemistry and Biological Chemistry, Faculty of Engineering, Kyoto University, PRESTO, JST, Kyoto 606-8501, Japan

Received: December 12, 2003; In Final Form: February 13, 2004

A recent experimental report on the suppression of the oxidative decomposition of guanines in deoxyribonucleic acid (DNA) double helices due to the attachment of a phenyl group to a guanine [Nakatani, K.; Dohno, C.; Saito, I. *J. Am. Chem. Soc.* **2002**, *124*, 6802] is examined by semiempirical Hartree−Fock (HF) molecular orbital (MO) calculations and ab initio HF MO calculations with the STO-3G basis set. Because of this attachment, the energy level of MO localized on the guanine shifts to lower energy in a vacuum, whereas it shifts to higher energy in water. This is mainly because the energy reduction of MO levels by the water solvent becomes smaller when the solvent molecules are excluded by the phenyl group. Consequently, a hole trap is enhanced at the phenylated guanine base in water. The observed suppression of the oxidative decomposition of guanines around the phenylated guanine is thus explained by considering the solvent effects. In addition, we have observed that energy shifts due to a benzyl group or a *tert*-butyl group are similar to those due to the phenyl group in our calculation.

1. Introduction

Deoxyribonucleic acid (DNA) is one of the candidates for next-generation electronic devices,[1] because of the full controllability of its sequence, the self-assembling feature, and the conducting properties. Especially, the conducting properties of DNA have attracted much attention in recent years and numerous experimental studies have been reported.[2−6] However, there are some obstacles to use DNA as a molecular device. One of the obstacles is the oxidative decomposition; i.e., DNA can easily be oxidized and subsequently decomposed at the guanine bases.[2,6−13] Recently, it has been reported that the oxidative decomposition is dramatically suppressed by attaching a phenyl group to a guanine in a double-stranded oligodeoxynucleotide (ODN).[14] To suppress the oxidative decomposition further, it is important to understand the role of N^2-phenyldeoxyguanosine in DNA.

Stimulated by the experimental studies, theoretical analysis of the conducting properties of DNA has been performed by many groups.[15−33] For those analyses, the electronic structure calculation gives a lot of information that is related to the energetics and kinetics.[28−33] For the study of the electronic structure of DNA, it is important to include the solvent effect. However, most of the earlier calculations of the electronic structure of DNA are conducted in a vacuum, mainly because the calculation including the solvent effect for this large molecule is computationally demanding. As small fragments of DNA, the solvent effect on the ionization potential of nucleotides and a phosphorylated dinucleotide with counterions has been studied intensively.[29,30] More recently, much-larger-sized DNA systems have been studied including the solvent effect.[31−33] These studies further confirm the importance of the solvent effect on the electronic properties of DNA.

In this paper, we analyze the energetics of the phenyl group attachment to a guanine. One of the interesting results found in ref 14 is that the oxidative decomposition is suppressed not only at the phenylated guanine but also at the guanines around the phenylated one. If the role of the phenyl group is only to suppress the deprotonation of the phenylated guanine radical cation,[8,34−36] a hole at the phenylated guanine has a greater chance to be transferred to the neighboring guanine bases and their oxidative decomposition will increase, which contradicts the experimental observation.[14] To explain the experimental results, we must examine energetics of this system. Here, we perform semiempirical Hartree−Fock (HF) molecular orbital (MO) calculations and ab initio HF MO calculations with the STO-3G basis set and find that the energy level of MO localized on the guanine shifts to lower energy in a vacuum, whereas it shifts to higher energy in water because of the attachment of a phenyl group to a guanine. This is mainly because the energy reduction of MO levels by the water solvent becomes smaller when the solvent molecules are excluded by the phenyl group. Consequently, a hole trap is enhanced at the phenylated guanine base in water and guanines around the phenylated one have fewer chances to trap a hole. The observed suppression of the

* Author to whom correspondence should be addressed. E-mail address: aokada@ims.tsukuba.ac.jp.
[†] JST.
[‡] University of Tsukuba.
[§] Toyohashi University of Technology.
[⊥] Toshiba R&D Center.
[||] Kyoto University, PRESTO.

10.1021/jp037845s CCC: $27.50
Published on Web 05/04/2004

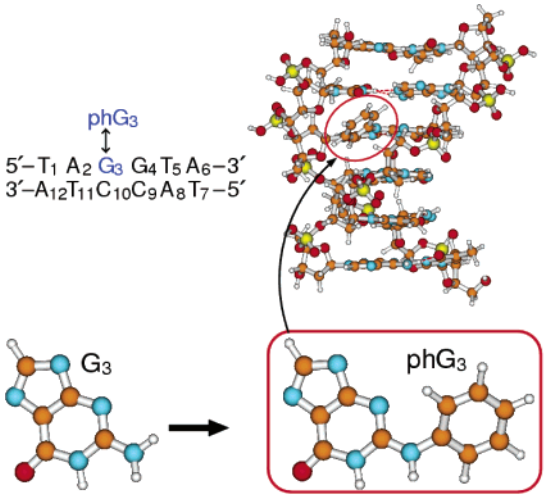

Figure 1. Structure of ODN ^{Ph}GG. The numbers of atoms of ODN GG and ODN ^{Ph}GG are 390 and 400, respectively. The approximate dimension of ODN GG is given as follows: (1) the distances between the two P atoms located between the stacked Watson−Crick base pairs are 17.76 and 18.21 Å for the 4th and 55th fiber model structures, respectively; (2) the distances between the N1 site of the adenine at each end of ODN GG are 16.85 and 16.98 Å for the 4th and 55th fiber model structures, respectively.

oxidative decomposition of guanines around the phenylated guanine[14] is thus explained by the solvent effects on the energetics of DNA.

The paper is organized as follows. In Section 2, we explain the methods in our calculations, such as the preparation of the DNA structure, semiempirical and ab initio HF MO calculations, and solvent models. In Section 3, the energy shift due to the phenyl group attachment to a guanine in a double-stranded ODN is shown as a main result. To assess the validity of our calculations, we also show the results with other models, i.e., other semiempirical HF MO calculations, and ab initio HF MO calculations with the STO-3G basis set. We then explain the relation between the energy shift and the observed suppression of the oxidative decomposition of guanines around the phenylated guanine.[14] To clarify the origin of the energy shift, the result is compared to the calculation of DNA with a H_2 cluster (10 H_2 molecules) in place of the phenyl group, where the H_2 cluster mimics the solvent-accessible surface of the phenyl group. The solvent effect is further examined for DNA molecules with other functional groups attached: a benzyl-group-attached DNA and a *tert*-butyl-group-attached DNA. Finally, conclusions are given in Section 4.

2. Methods

The sequence 5′-TAGGTA-3′ and its phenylated counterpart 5′-TA^{Ph}GGTA-3′ appear as a part of the oligomers investigated in ref 14. We denote the former as ODN GG and latter as ODN ^{Ph}GG (see Figure 1). The B-DNA structure of ODN GG with backbones is constructed by the 3DNA v1.5 program.[37] To ensure that our conclusion is not dependent on the structure, we have chosen two typical B-DNA structures in the calculation, i.e., the 4th[38] and 55th[39] fiber models (see Tables S1 and S10 in the Supporting Information). These fiber models are determined by X-ray diffraction analysis. Therefore, only the positions of the heavy atoms are identified. H atoms are attached, and their positions are optimized using Austin Model 1 (AM1)[40] in the MOPAC2002 v1.0 program.[41] (We do not use the linear scaling calculation program MOZYME that is implemented in MOPAC2002.) The geometry optimization of the H atoms in the water solvent is performed by AM1 with the conductor-like screening model (COSMO).[42,43] The structure of ODN ^{Ph}GG is obtained by attaching the phenyl group to ODN GG and optimizing the geometry of the phenyl group by AM1 (AM1/COSMO) in a vacuum (water). Both the 4th and 55th fiber models have similar global structural parameters; i.e., the helical twists are 36° for both fiber models, and the rises are 3.38 and 3.39 Å for the 4th and 55th fiber models, respectively. The structural differences between these two fiber models are mainly found in the sugar−phosphate backbone parameters. The structures used in the calculations are given in Tables S1−S18 in the Supporting Information.

TABLE 1: Differences in Vertical Ionization Potentials (IPs) between Guanine and other DNA Bases, and Differences in Oxidation Potentials (OPs) between Deoxyguanosine and Other Nucleosides[a]

	IP (eV)			OP (V)		
				AM1		
	AM1	experiment[b]		optimized vdW radii[c]	default vdW radii[d]	experiment
A	0.09	0.20	dA	0.23	0.16	0.49[e]
C	0.70	0.70	dC	0.76	0.63	0.65[e]
T	0.93	0.90	dT	0.73	0.58	0.62[e]
			d^{ph}G	−0.01	−0.17	0.03[f]

[a] The geometries are optimized by AM1. [b] Data from ref 44. [c] Data from ref 43. [d] Data from ref 41. [e] Data from ref 45. [f] Data from ref 14.

The electronic structure calculation is performed by the AM1 Hamiltonian[40] implemented in a semiempirical MO program MOPAC2002.[41] The solvent effect is taken into account by a continuum solvent model, i.e., COSMO.[42,43] We use the Koopmans theorem to examine the energy shifts of MO energy levels near the highest occupied molecular orbital (HOMO) of ODNs. The use of this method is justified in the following.

(1) As for the validity of the Koopmans theorem with AM1 and COSMO, we calculate the relative ionization potentials (IPs) for bases in a vacuum and the relative oxidation potentials (OPs) for nucleosides in water and compare them to experiments. The root-mean-square (RMS) deviations between computational and experimental results[14,44,45] are 0.07 eV and 0.15 V (Table 1) for IPs and OPs, respectively.

(2) The aforementioned energy shifts obtained by the Koopmans theorem do not include the difference of the reorganization energies between the guanine and phenylated guanine. However, this difference, as evaluated from the experimental results,[46] is less than ∼0.13 eV (see Appendix for details). These values are smaller than the energy change that is due to the attachment of the phenyl group obtained by the Koopmans theorem and, therefore, do not change our conclusion.

Our conclusions obtained uisng the AM1/COSMO calculations are further confirmed by different models, i.e., (i) the MNDO−Parametric Method 3 (PM3) Hamiltonian[47] with the COSMO in MOPAC2002 and (ii) the generalized Born (GB) model[48] implemented in ABINIT/GB, which is an ab initio MO/GB program package.[49] The PM3 calculation is performed in a manner similar to that for the AM1 calculation, except that the geometries of H atoms and the phenyl group are optimized by PM3. The ABINIT/GB calculations are performed with the STO-3G basis set. We use the 4th fiber model structure, and the geometries of H atoms and the phenyl group are optimized by AM1.

The parameters used for the COSMO calculation are given as follows. The dielectric constant of water is taken as $\epsilon = 78.4$. Because the van der Waals (vdW) parameters of COSMO

implemented in MOPAC2002 are not optimized, we use the optimized vdW parameters of COSMO for the density functional formalism (DFT) calculation.[43] Those optimized vdW parameters are expected to produce better results than the default vdW parameters of COSMO[50] (see the Supporting Information). In fact, the RMS deviation between the experimental relative OPs[14,45] and the computational OPs with the default vdW parameters of COSMO in MOPAC2002[41] is 0.19 V, which is larger than that with the optimized vdW parameters (i.e., 0.15 V; see Table 1). Among the optimized vdW radii, the vdW radius for the P atom is not reported in ref 43. Instead, we use a suggested value of 2.106 Å as the vdW radius for the P atom.[50] To assess whether the results in the following are unaffected by the vdW radius of the P atom, we have also performed the calculations for different vdW radii of the P atom (i.e., 1.906 and 2.306 Å) and found that the results change little.

We report the results of the neutral DNA in water and in a vacuum in the following, because the positions of the counterions have been observed to have little effect on the energy differences between the HOMO and other occupied MOs near the HOMO in the calculations including the water solvent as follows. The calculations in the water solvent have been performed by considering ODN GG (ODN ^{Ph}GG) in both neutral and ionic states. The calculations of ODN GG (ODN ^{Ph}GG) in ionic states have been performed by eliminating 10 H atoms at the phosphate backbones and assigning the total charge of −10. Our ionic state calculation corresponds to the case where the counterions are far away from the DNA molecule, compared to the solvent layers that are surrounding the DNA molecule. The actual DNA molecule in an ionic state should be between the neutral and our ionic state calculations. Our ionic state calculation only gives mere energy shifts of 0.26−0.32 eV (see Table S19 in the Supporting Information) for the occupied levels near the HOMO, compared to the neutral one; i.e., the energy differences between the HOMO and other occupied MOs near the HOMO change little between the DNA in ionic and neutral states in water (see Table S19 in the Supporting Information).

This can be understood as follows. We note here that the first several occupied MOs near the HOMO of ODN GG in water are all localized on bases. The energy levels of MOs localized on a phosphate group are more than 1 eV lower than the energy level of HOMO in the water solvent, which is consistent with refs 29 and 30. Because the charge around the phosphate group is surrounded by the solvent water, its electrostatic effect on the MOs localized on bases is shielded. The magnitude of the energy shifts is consistent with the difference between the calculated IPs of a phosphorylated dinucleotide with and without Na^+ cations in solution.[30]

The geometries of the heavy atoms of ODN GG and ODN ^{Ph}GG (except the phenyl group) are not optimized in our calculations. (The geometries of the H atoms are optimized in both cases.) This is justified as follows. To see the effect of a geometry optimization, we compare IPs of a guanine with and without the geometry optimization by AM1 for heavy atoms. We are only interested in the energy shift that is due to the attachment of the phenyl group to the guanine; therefore, the difference of IPs between the guanine and phenylated guanine is important. The change of the geometry causes a change of the difference of IPs between the guanine and phenylated guanine where the geometry of the heavy atoms of a guanine is extracted from the fiber model structure, i.e., 0.05 and 0.04 eV for the 4th and 55th fiber model structures, respectively. The energy change due to the attachment of the phenyl group obtained by the Koopmans theorem is larger than those values.

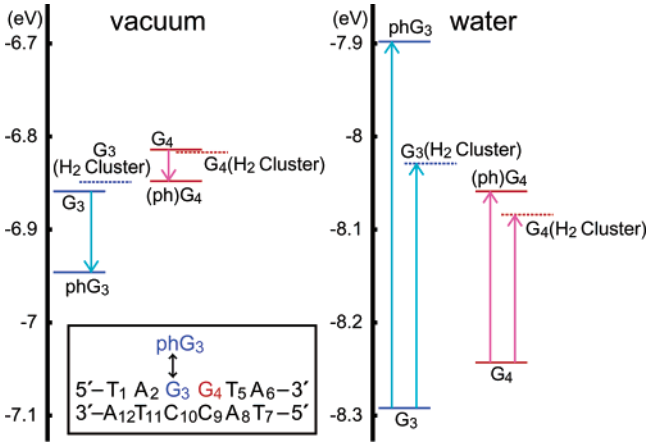

Figure 2. Energy shifts near the HOMO levels by the attachment of a phenyl group to G_3 with the 4th fiber model structure. Blue lines are for the energy levels of the G_3 localized orbitals, and red lines are for the energy levels of the G_4 localized orbitals. The energy levels of the DNA−H_2 cluster system, where the H_2 cluster mimics the solvent exclusion effect of the phenyl group (see Figure 4), are shown with dashed lines. The AM1/COSMO method is used. The energy level of MO localized on G_3 shifts to lower energy in a vacuum (left panel). In contrast, the same energy level shifts to higher energy in water (right panel). Inset shows the sequence of investigated double-stranded DNA.

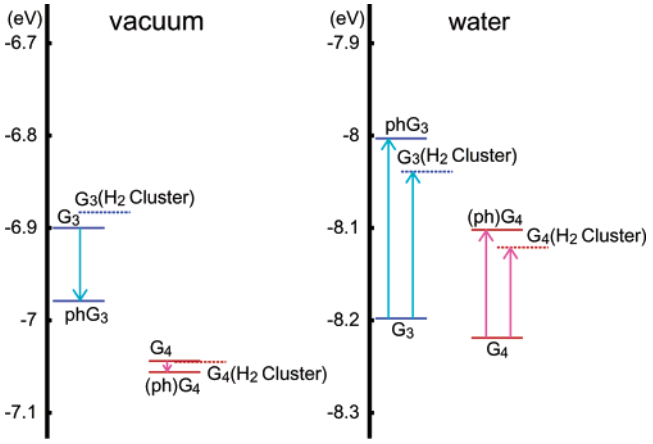

Figure 3. Energy shifts near the HOMO levels by the attachment of a phenyl group to G_3 with the 55th fiber model structure. Blue lines are for the energy levels of the G_3 localized orbitals, and red lines are for the energy levels of the G_4 localized orbitals. The energy levels of the DNA−H_2 cluster system, where the H_2 cluster mimics the solvent exclusion effect of the phenyl group (see Figure 4), are shown with dashed lines. The AM1/COSMO method is used. The energy level of MO localized on G_3 shifts to lower energy in a vacuum (left panel). In contrast, the same energy level shifts to higher energy in water (right panel). Inset shows the sequence of investigated double-stranded DNA.

3. Results and Discussion

3.1. Energy Shift of Molecular Orbital (MO) Localized on Guanine because of Phenyl Group Attachment and Comparison with Experiment. First, we show the results of the electronic structure calculation by AM1 with the COSMO model. The HOMO and HOMO-1 energy levels are shown in Figures 2 and 3. The bases that have the largest coefficients of the HOMO and HOMO-1 are indicated near the MO energy levels. (The MOs are highly localized on a base except ODN GG in water. The Coulomb interaction is strongly shielded in water; thus, the sequence dependence of the potential on each base due to the Coulomb interaction is rather suppressed. Therefore, the energy levels of G_3 and G_4 in water are almost degenerate and its HOMO and HOMO-1 levels are delocalized

TABLE 2: Energy Levels (in eV) of G_3 and G_4 Localized Orbitals of ODN GG and ODN ^{Ph}GG for the 4th and 55th Fiber Model Structures[a]

	vacuum		water	
	ODN GG	ODN ^{Ph}GG	ODN GG	ODN ^{Ph}GG
	4th fiber model			
G_3	−6.58	−6.64 (−0.05)	−8.11	−7.68 (0.43)
G_4	−6.75	−6.76 (−0.01)	−8.13	−7.91 (0.22)
	55th fiber model			
G_3	−6.67	−6.71 (−0.04)	−8.05	−7.80 (0.25)
G_4	−6.84	−6.89 (−0.05)	−8.08	−7.97 (0.11)

[a] The number in parentheses shows the energy shift (in eV) compared to the energy levels of ODN GG. The PM3/COSMO method is used.

TABLE 3: Energy Levels (in eV) of G_3 and G_4 Localized Orbitals of ODN GG and ODN ^{Ph}GG for the 4th Fiber Model Structure[a]

	vacuum		water	
	ODN GG	ODN ^{Ph}GG	ODN GG	ODN ^{Ph}GG
G_3	−3.925	−3.967 (−0.042)	−5.115	−5.039 (0.076)
G_4	−3.817	−3.850 (−0.033)	−5.002	−4.992 (0.010)

[a] The number in parentheses shows the energy shift (in eV) compared to the energy levels of ODN GG. The GB model implemented in the ab initio MO calculation program ABINIT/GB with the STO-3G basis set is used.

over those two bases.) Figures 2 and 3 indicate that attachment of a phenyl group to G_3 causes the following energy shifts of the HOMO and HOMO-1: (i) in a vacuum, the energy level of the G_3 localized orbital shifts to lower energy and the energy level of the G_4 localized orbital changes little, whereas (ii) in water, the energy levels of the localized orbitals of both G_3 and G_4 shift to higher values. The magnitude of change is larger for G_3. Consequently, the HOMO is localized on the phenylated guanine.

In addition, we have examined the solvent effect by different models, i.e., (i) the PM3 Hamiltonian[47] with the COSMO model in MOPAC2002 and (ii) the GB model[48] implemented in the ab initio MO/GB program package ABINIT/GB.[49] The ABINIT/GB program has been successfully applied to many systems (see, for example, ref 51). The PM3 calculation is conducted in a manner similar to that of the AM1 calculation explained in Section 2, except that the geometries of the H atoms and the phenyl group are optimized by the PM3 Hamiltonian. The energy shifts calculated by PM3 (Table 2) are very similar to those calculated by AM1 (see Figures 2 and 3). The ABINIT/GB calculations are performed with the STO-3G basis set. We use the 4th fiber model structure, and the geometries of the H atoms and the phenyl group are optimized by AM1. The energy shifts in Table 3 are again similar to those obtained by the AM1 calculations. These different types of calculations further confirm that the energy level of MO localized on G_3 shifts to higher value in water because of the attachment of a phenyl group to a guanine.

Experimentally, it has been observed that the introduction of N^2-phenyldeoxyguanosine significantly suppresses the oxidative decomposition at the phenylated base as well as other guanine bases.[14] Because the electronic energy levels of the phenylated guanine are higher than those of other guanine bases, the phenylated guanine has a greater chance to trap a hole than other guanine bases, which leads to the suppression of the oxidative decomposition of the guanine bases other than the phenylated one. The trapped hole experiences the annihilation processes

TABLE 4: Charge Distributions of HOMO, Which is Localized on the PhG_3[a]

	vacuum		water	
	G_3	phenyl group	G_3	phenyl group
4th fiber model	0.91	0.06	0.75	0.25
55th fiber model	0.94	0.05	0.89	0.10

[a] The AM1/COSMO method is used.

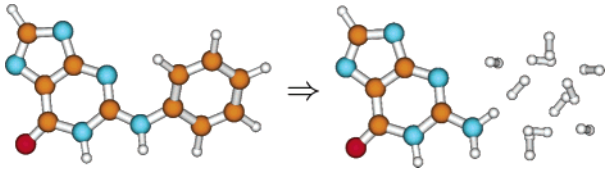

Figure 4. Structure of the H_2 cluster.

afterward, which results in the suppression of oxidative decomposition of the phenylated guanine.[14]

3.2. Origin of Energy Shift due to the Phenyl Group and Cases of Benzyl Group and *tert*-Butyl Group. The energy shifts shown in Section 3.1 are mainly due to the following two reasons: (i) the very existence of phenyl group prevents water molecules from approaching DNA, especially near the phenylated base; and (ii) attachment of a phenyl group to the guanine causes charge transfer between the phenyl group and guanine (see Table 4). To better understand them, we have conducted AM1/COSMO calculations of DNA with a H_2 cluster (10 H_2 molecules) in place of the phenyl group, where the H_2 cluster mimics the solvent-accessible surface of the phenyl group (see Figure 4). The geometry of the H_2 cluster is determined only from the geometry of the phenyl group, i.e., two H_2 molecules are assigned for each C−H of the phenyl group where one of four H atoms is placed at the position of the H atom of C−H and other three H atoms are placed around the C atom of C−H (see Tables S6, S9, S15, and S18 in the Supporting Information). Because there is little mixing between the MOs of G_3 and those of the H_2 cluster, we can selectively observe the effect of the exclusion of the solvent. The energy levels with the H_2 cluster are indicated by dashed lines in Figures 2 and 3. In a vacuum, the energy levels of the HOMO and HOMO-1 of the ODN GG-H_2 cluster system are very similar to those of ODN GG. This is expected because the existence of the H_2 cluster should have little effect on the energy levels of DNA. In water, on the other hand, the energy shift due to the H_2 cluster is similar to the shift due to the phenyl group, especially for the G_4 localized orbital. Because there is little charge transfer from G_4 to the phenyl group, the energy shifts of the G_4 localized orbital due to the phenyl group and the H_2 cluster are of the same origin, i.e., the solvent exclusion effect. In the case of the G_3 localized orbital, there is an additional effect on the energy shift due to charge transfer between the phenyl group and guanine (see Table 4). This may be the reason for the discrepancies between the energy shifts by the phenyl group and the H_2 cluster.

To further confirm the solvent exclusion effect, we have performed AM1/COSMO calculations of a DNA molecule with a benzyl group ($-CH_2C_6H_5$) attached instead of one with a phenyl group attached (i.e., a CH_2 spacer is inserted between the guanine and the phenyl group). We then compare the results to the corresponding DNA−H_2 cluster calculations (see Table 5). There is little charge transfer between the guanine and the phenyl group, because of the spacer. Therefore, we can expect that the MO energy levels near the HOMO without the benzyl group are similar to those with the H_2 cluster in a vacuum,

TABLE 5: Energy Levels (in eV) of G_3 and G_4 Localized Orbitals of ODN GG and a Benzyl-Group-Attached ODN GG, Which is Denoted as ODN ^{Bz}GG, for the 4th and 55th Fiber Model Structures[a]

	vacuum			water		
	ODN GG	ODN ^{Bz}GG	ODN GG + H_2 cluster	ODN GG	ODN ^{Bz}GG	ODN GG + H_2 cluster
			4th fiber model			
G_3	−6.86	−6.91 (−0.05)	−6.86 (0.00)	−8.29	−8.01 (0.28)	−8.03 (0.26)
G_4	−6.81	−6.96 (−0.15)	−6.82 (−0.01)	−8.24	−8.15 (0.09)	−8.10 (0.14)
			55th fiber model			
G_3	−6.90	−6.98 (−0.08)	−6.89 (0.01)	−8.20	−8.00 (0.20)	−8.03 (0.17)
G_4	−7.04	−7.16 (−0.12)	−7.05 (−0.01)	−8.22	−8.16 (0.06)	−8.13 (0.09)

[a] The energy levels (eV) of the ODN GG−H_2 cluster system, where the H_2 cluster mimics the solvent exclusion effect of the benzyl group, are also shown. The number in parentheses shows the energy shift (in eV) compared to the energy levels of ODN GG. The AM1/COSMO method is used.

TABLE 6: Energy Levels (in eV) of G_3 and G_4 Localized Orbitals of ODN GG and a *tert*-Butyl-Group-Attached ODN GG, Which is Denoted as ODN $^{t-Bu}$GG, for the 4th and 55th Fiber Model Structures[a]

	vacuum		water	
	ODN GG	ODN $^{t-Bu}$GG	ODN GG	ODN $^{t-Bu}$GG
		4th fiber model		
G_3	−6.86	−6.75 (0.11)	−8.29	−7.92 (0.37)
G_4	−6.81	−6.83 (−0.02)	−8.24	−8.08 (0.16)
		55th fiber model		
G_3	−6.90	−6.83 (0.07)	−8.20	−7.94 (0.26)
G_4	−7.04	−7.00 (0.04)	−8.22	−8.07 (0.15)

[a] The number in parentheses shows the energy shift (in eV) compared to the energy levels of ODN GG. The AM1/COSMO method is used.

whereas those with the benzyl group are similar to those with the H_2 cluster in water, because of the solvent exclusion effect. The results show that this is indeed the case. In water, the energy differences between the two HOMOs with the benzyl group and with the H_2 cluster are <0.02 eV (see Table 5). Please note that rather large energy shifts are found for G_4, because of the geometry of the benzyl group. For the 4th fiber model, the closest distance between the H atom in G_4 and the H atom in the benzyl group is 2.02 Å after the geometry optimization for the benzyl group by AM1.

If the large part of the energy shift is due to the solvent exclusion effect, a similar energy shift is expected by attaching an alkyl group to a guanine in a double-stranded ODN. Therefore, we have performed AM1/COSMO calculations of DNA with a *tert*-butyl group attached (i.e., the phenyl group is replaced by the *tert*-butyl group). As is expected, the energy shifts in water (Table 6) are similar to those with phenylated guanine (see Figures 2 and 3). On the other hand, unlike the phenylated case, the energy level of the G_3 localized orbital in a vacuum shifts to higher energy by ∼0.1 eV. However, our assertion about the energy shift due to the solvent exclusion effect is still valid, because the energy shifts are larger in water than in a vacuum, by 0.27 and 0.19 eV in the 4th and 55th fiber model structures, respectively.

The reason for the energy shift to higher energy because of the solvent exclusion effect can be explained as follows. The MO levels near the HOMO of B-DNA shift to the lower energy in water compared to that in a vacuum. This is consistent with the finding that the energy levels of occupied MOs near the HOMO of a phosphorylated dinucleotide in a vacuum shift to lower energy in water.[30] (Note the difference of the energy levels for vacuum and for water in Figures 2 and 3.) When the phenyl group is attached to a base, the nearby bases experience a weaker solvent effect. As a result, the localized orbitals around the phenylated base shift to higher energies.

4. Conclusions

In conclusion, the energy level of a molecular orbital (MO) localized on a guanine shifts to lower value in a vacuum but to higher value in water, when a phenyl group is attached to the guanine base in a double-stranded DNA. This is mainly because the energy reduction of MO levels by the water solvent becomes smaller when the solvent is excluded by the phenyl group. As a result, we can expect that a phenylated guanine base has a greater chance to trap a hole in water. The observed suppression of the oxidative decomposition of guanines around the phenylated guanine[14] is thus explained in terms of the solvent effects. In addition, we have determined that the energy shifts due to the benzyl group or the *tert*-butyl group are similar to those that are due to the phenyl group in our calculation.

Supporting Information Available: Parameters used in the COSMO calculations; geometry used in the calculations (Tables S1−S18); comparison of the energy levels between DNA in neutral and ionic states in solution (Table S19). (PDF.) This material is available free of charge via the Internet at http://pubs.acs.org.

Acknowledgment. We are grateful to Dr. A. Klamt for the suggestions for the van der Waals parameters of COSMO. We are also thankful to Dr. T. Watanabe for his help related to the ABINIT/GB package. This research is supported by "Research and Development for Applying Advanced Computational Science and Technology" of Japan Science and Technology Corporation (ACT-JST).

Appendix: Evaluation of the Reorganization Energies

Let us denote the reorganization energy of a guanine base as λ_i^G and the solvent reorganization energy around the guanine as λ_s^G when a hole is injected to the guanine. The total reorganization energy around the guanine base λ^G then is given by

$$\lambda^G = \lambda_s^G + \lambda_i^G \tag{A1}$$

Similarly, we have

$$\lambda^{phG} = \lambda_s^{phG} + \lambda_i^{phG} \simeq \lambda_s^{phG} + \lambda_i^G + \lambda_i^{ph} \tag{A2}$$

Here, we assume that the reorganization energy of the phenylated guanine λ_i^{phG} can be approximated by the sum of λ_i^G and the reorganization energy of phenyl group λ_i^{ph}. Therefore, the difference of the reorganization energy between guanine and phenylated guanine is given by

$$\lambda^G - \lambda^{phG} \simeq \lambda_s^G - (\lambda_s^{phG} + \lambda_i^{ph}) \tag{A3}$$

The solvent reorganization energy of a DNA with a donor (guanine), an acceptor (diol), and a bridge has been reported as $\lambda_s = 0.27$ eV.[46] Because the diol is exposed to the solvent, the solvent reorganization energy around the donor is larger than that around the acceptor. Therefore, the reorganization energy due to the solvent around the guanine (λ_s^G) is expected to be less than a half of λ_s. When the phenyl group is attached to the guanine, the solvent reorganization energy λ_s^{phG} is smaller than λ_s^G. The energy reduction is partially compensated by the reorganization energy of the phenyl group (λ_i^{ph}). As a result, the change of the reorganization energy that is due to the attachment of the phenyl group to the guanine (eq A3) is expected to be <0.13 eV.

References and Notes

(1) Dekker, C.; Ratner, M. A. *Phys. World* **2001**, *14*, 29.

(2) (a) Grinstaff, M. W. *Angew. Chem., Int. Ed.* **1999**, *38*, 3629. (b) Schuster, G. B. *Acc. Chem. Res.* **2000**, *33*, 253. (c) Giese, B. *Acc. Chem. Res.* **2000**, *33*, 631.

(3) Lewis, F. D.; Letsinger, R. L.; Wasielewski, M. R. *Acc. Chem. Res.* **2001**, *34*, 159.

(4) (a) Porath, D.; Bezryadin, A.; de Vries, S.; Dekker, C. *Nature* **2000**, *403*, 635. (b) Yoo, K.-H.; Ha, D. H.; Lee, J.-O.; Park, J. W.; Kim, J.; Kim, J. J.; Lee, H.-Y.; Kawai, T.; Choi, H. Y. *Phys. Rev. Lett.* **2001**, *87*, 198102. (c) Watanabe, H.; Manabe, C.; Shigematsu, T.; Shimotani, K.; Shimizu, M. *Appl. Phys. Lett.* **2001**, *79*, 2462.

(5) (a) Fukui, K.; Tanaka, K. *Angew. Chem., Int. Ed.* **1998**, *37*, 158. (b) Kawai, K.; Takada, T.; Tojo, S.; Ichinose, N.; Majima, T. *J. Am. Chem. Soc.* **2001**, *123*, 12688. (c) Fukuzumi, S.; Nishimine, M.; Ohkubo, K.; Tkachenko, N. V.; Lemmetyinen, H. *J. Phys. Chem. B* **2003**, *107*, 12511.

(6) (a) Gasper, S. M.; Schuster, G. B. *J. Am. Chem. Soc.* **1997**, *119*, 12762. (b) Hall, D. B.; Holmlin, R. E.; Barton, J. K. *Nature* **1996**, *382*, 731. (c) Núñez, M. E.; Hall, D. B.; Barton, J. K. *Chem. Biol.* **1999**, *6*, 85. (d) Nakatani, K.; Dohno, C.; Saito, I. *J. Am. Chem. Soc.* **1999**, *121*, 10854.

(7) (a) Saito, I.; Takayama, M.; Sugiyama, H.; Nakatani, K. *J. Am. Chem. Soc.* **1995**, *117*, 6406. (b) Sugiyama, H.; Saito, I. *J. Am. Chem. Soc.* **1996**, *118*, 7063.

(8) Yoshioka, Y.; Kitagawa, Y.; Takano, Y.; Yamaguchi, K.; Nakamura, T.; Saito, I. *J. Am. Chem. Soc.* **1999**, *121*, 8712.

(9) (a) Tanielian, C.; Kobayashi, M.; Wolff, C. *J. Biomed. Opt.* **2001**, *6*, 252. (b) Kobayashi, M.; Koyama, S.; Nakazato, M.; Miyoshi, N.; Wolff, C.; Daikuzono, N.; Tanielian, C.; Sasaki, M.; Komiyama, M. *J. Clin. Laser Med. Surg.* **1994**, *12*, 133.

(10) (a) Ito, K.; Inoue, S.; Yamamoto, K.; Kawanishi, S. *J. Biol. Chem.* **1993**, *268*, 13221. (b) Oikawa, S.; Tada-Oikawa, S.; Kawanishi, S. *Biochemistry* **2001**, *40*, 4763.

(11) Voityuk, A. A.; Jortner, J.; Bixon, M.; Rösch, N. *Chem. Phys. Lett.* **2000**, *324*, 430.

(12) Zhu, Q.; LeBreton, P. R. *J. Am. Chem. Soc.* **2000**, *122*, 12824.

(13) Prat, F.; Houk, K. N.; Foote, C. S. *J. Am. Chem. Soc.* **1998**, *120*, 845.

(14) Nakatani, K.; Dohno, C.; Saito, I. *J. Am. Chem. Soc.* **2002**, *124*, 6802.

(15) (a) Bixon, M.; Giese, B.; Wessely, S.; Langenbacher, T.; Michel-Beyerle M. E.; Jortner, J. *Proc. Natl. Acad. Sci. U.S.A.* **1999**, *96*, 11713. (b) Voityuk, A. A.; Rösch, N.; Bixon, M.; Jortner, J. *J. Phys. Chem. B* **2000**, *104*, 9740.

(16) (a) Berlin, Y. A.; Burin, A. L.; Ratner, M. A. *J. Am. Chem. Soc.* **2001**, *123*, 260. (b) Grozema, F. C.; Siebbeles, L. D. A.; Berlin, Y. A.; Ratner, M. A. *Chem. Phys. Chem.* **2002**, *3*, 536.

(17) Okada, A.; Chernyak, V.; Mukamel, S. *J. Phys. Chem. A* **1998**, *102*, 1241.

(18) Okada, A.; Yokojima, S.; Kurita, N.; Sengoku, Y.; Tanaka, S. *J. Mol. Struct.* (*THEOCHEM*) **2003**, *630*, 283.

(19) (a) Priyadarshy, S.; Risser, S. M.; Beratan, D. N. *J. Phys. Chem.* **1996**, *100*, 17678. (b) Tong, G. S. M.; Kurnikov, I. V.; Beratan, D. N. *J. Phys. Chem. B* **2002**, *106*, 2381.

(20) Felts, A. K.; Pollard, W. T.; Friesner, R. A. *J. Phys. Chem.* **1995**, *99*, 2929.

(21) Segal, D.; Nitzan, A. *Chem. Phys.* **2002**, *281*, 235.

(22) (a) Li, X.-Q.; Yan, Y. J. *Appl. Phys. Lett.* **2001**, *79*, 2190. (b) Yan, Y. J.; Zhang, H. *J. Theor. Comput. Chem.* **2002**, *1*, 225.

(23) Conwell, E. M.; Rakhmanova, S. V. *Proc. Natl. Acad. Sci. U.S.A.* **2000**, *97*, 4556.

(24) Asai, Y. *J. Phys. Chem. B* **2003**, *107*, 4647.

(25) Kurnikov, I. V.; Tong, G. S. M.; Madrid, M.; Beratan, D. N. *J. Phys. Chem. B* **2002**, *106*, 7.

(26) Tanaka, S.; Sengoku, Y. *Phys. Rev. E* **2003**, *68*, 031905.

(27) Renger, T.; Marcus, R. A. *J. Phys. Chem. A* **2003**, *107*, 8404.

(28) Yoshioka, Y.; Kawai, H.; Sato, T.; Yamaguchi, K.; Saito, I. *J. Am. Chem. Soc.* **2003**, *125*, 1968.

(29) Kim, N. S.; LeBreton, P. R. *J. Am. Chem. Soc.* **1996**, *118*, 3694.

(30) Kim, N. S.; Zhu, Q.; LeBreton, P. R. *J. Am. Chem. Soc.* **1999**, *121*, 11516.

(31) Starikov, E. B. *Phys. Chem. Chem. Phys.* **2002**, *4*, 4523.

(32) Gervasio, F. L.; Carloni, P.; Parrinello, M. *Phys. Rev. Lett.* **2002**, *89*, 108102.

(33) Reynisson, J.; Schuster, G. B.; Howerton, S. B.; Williams, L. D.; Barnett, R. N.; Cleveland, C. L.; Landman, U.; Harrit, N.; Chaires, J. B. *J. Am. Chem. Soc.* **2003**, *125*, 2072.

(34) Kino, K.; Saito, I.; Sugiyama, H. *J. Am. Chem. Soc.* **1998**, *120*, 7373.

(35) Cadet, J.; Berger, M.; Buchko, G. W.; Joshi, P. C.; Raoul, S.; Ravanat, J.-L. *J. Am. Chem. Soc.* **1994**, *116*, 7403.

(36) Vialas, C.; Pratviel, G.; Claparols, C.; Meunier, B. *J. Am. Chem. Soc.* **1998**, *120*, 11548.

(37) Lu, X.-J.; Shakked, Z.; Olson, W. K. *J. Mol. Biol.* **2000**, *300*, 819.

(38) (a) Arnott, S. Polynucleotide Secondary Structures: An Historical Perspective. In *Oxford Handbook of Nucleic Acid Structure*; Neidle, S., Ed.: Oxford University Press: New York, 1999; pp 1−38. (b) Chandrasekaran, R.; Arnott, S. *J. Biomol. Struct. Dyn.* **1996**, *13*, 1015.

(39) Premilat S.; Albiser, G. *Nucleic Acids Res.* **1983**, *11*, 1897.

(40) (a) Dewar, M. J. S.; Zoebisch, E. G.; Healy, E. F.; Stewart, J. J. P. *J. Am. Chem. Soc.* **1985**, *107*, 3902. (b) Dewar, M. J. S.; Jie, C. *J. Mol. Struct.* (*THEOCHEM*) **1989**, *187*, 1.

(41) Stewart, J. J. P., Fujitsu Limited, Tokyo, Japan, 2001.

(42) Klamt, A.; Schüürmann, G. *J. Chem. Soc., Perkin Trans.* **1993**, *2*, 799.

(43) Klamt, A.; Jonas, V.; Bürger, T.; Lohrenz, J. C. W. *J. Phys. Chem. A* **1998**, *102*, 5074.

(44) Hush, N. S.; Cheung, A. S. *Chem. Phys. Lett.* **1975**, *34*, 11.

(45) Seidel, C. A. M.; Schulz, A.; Sauer, M. H. M. *J. Phys. Chem.* **1996**, *100*, 5541.

(46) Lewis, F. D.; Kalgutkar, R. S.; Wu, Y.; Liu, X.; Liu, J.; Hayes, R. T.; Miller, S. E.; Wasielewski, M. R. *J. Am. Chem. Soc.* **2000**, *122*, 12346.

(47) Stewart, J. J. P. *J. Comput. Chem.* **1989**, *10*, 209.

(48) (a) Born, M. *Z. Phys.* **1920**, *1*, 45. (b) Hoijtink, G. J.; de Boer, E.; van der Meij, P. H.; Weijland, W. P. *Recl. Trav. Chim. Pay−Bas.* **1956**, *75*, 487. (c) Jano, I. *C. R. Acad. Sci.* **1965**, *261*, 103.

(49) Kikuchi, O.; Morihashi, K.; Takahashi, O.; Nakano, T.; Ogawa, Y.; Inadomi, Y. ABINIT/GB, Ab Initio MO/GB Program Package; University of Tsukuba: Tsukuba, Japan, 1999.

(50) Klamt, A., personal communication.

(51) (a) Kikuchi, O.; Watanabe, T.; Ogawa, Y.; Takase, H.; Takahashi, O. *J. Phys. Org. Chem.* **1997**, *10*, 145. (b) Watanabe, T.; Hashimoto, K.; Takase, H.; Kikuchi, O. *J. Mol. Struct.* (*THEOCHEM*) **1997**, *397*, 113.